SAE TECHNICAL PAPER SERIES

2007-01-1303

Crank Angle - Based Diesel Engine Modeling for Hardware-in-the-Loop Applications with In-Cylinder Pressure Sensors

Tino Schulze, Markus Wiedemeier and Herbert Schuette
dSPACE GmbH - Germany

Reprinted From: Modeling of SI and Diesel Engines, 2007 (SP-2079)

ISBN 0-7680-1636-3

9 780768 016369

2007 World Congress
Detroit, Michigan
April 16-19, 2007

SAE International™

400 Commonwealth Drive, Warrendale, PA 15096-0001 U.S.A. Tel: (724) 776-4841 Fax: (724) 776-0790 Web: www.sae.org

All SAE papers, standards, and selected books are abstracted and indexed in the Global Mobility Database.

ISSN 0148-7191

Printed in USA

2007-01-1303

Crank Angle - Based Diesel Engine Modeling for Hardware-in-the-Loop Applications with In-Cylinder Pressure Sensors

Tino Schulze, Markus Wiedemeier and Herbert Schuette
dSPACE GmbH - Germany

ABSTRACT

Mean value engine models (MVEM) can be considered the standard models for hardware-in-the-loop (HIL) test systems for engine control units (ECUs). Mainly due to stricter environmental regulation, future ECUs for Diesel engines will also be equipped with in-cylinder pressure sensors. HIL test systems therefore have to provide the in-cylinder pressure in real time by means of a corresponding model. The paper describes extensions to an MVEM implemented in Simulink in order to calculate the in-cylinder pressure and temperature by means of appropriate heat release functions. Some emphasis is placed on the comparison of different heat release functions with respect to their applicability in real-time, closed-loop simulations. Some first steps in the calibration/parameterization of the chosen model based on real dynamometer measurements, along with a test on a real ECU, will complete this contribution.

INTRODUCTION

Real-time-capable mean value engine models (MVEM) are today well established in hardware-in-the-loop (HIL) systems for testing engine control units. These models can generate consistent sensor values like engine torque and speed, air mass flow, etc., according to the currently applied actuator controls, like injection, EGR rate, boost pressure control, etc. All sensor values are mean values, i. e., they do not reflect the cyclic characteristics of the combustion of the individual cylinders, but rather provide sensor values as a mean over 720 degrees crank angle.

In order to further improve fuel economy and emissions along with higher power, the next generation of Diesel ECUs will be equipped with in-cylinder pressure measurement. The in-cylinder pressure, obtained for example by a glow plug-integrated pressure transducer, will be used for essential control loops like engine torque control and cylinder balancing, and especially for Diesel engine controls, to reduce soot and NO_x significantly.

Since the injection pattern has a direct effect on Diesel combustion and therefore also on the cylinder pressure, MVEMs are no longer sufficient for closed-loop testing of the new ECU generation. Precise real-time calculation of the cylinder pressure according to the actual injection is needed. With this more detailed modeling approach, it is also possible to cope efficiently with variable valve timing, mainly used in gasoline engines, which typically could only be done approximately with MVEMs, relying on volumetric efficiency tables instead of modeling the mass flow through intake/exhaust valves.

After a short overview of the standard MVEMs, the paper describes in detail a Diesel engine model which is used in an HIL test system and which provides the cylinder pressure and temperature. Different approaches to combustion simulation (heat-release functions) will be discussed to show how appropriate they are with regard to HIL applications and I/O issues.

The comprehensive Simulink model structure comprising air path, turbocharger, EGR, common-rail injection system, etc., and implementation on a state-of-the-art real-time system are described. Special emphasis is placed on the interconnection of the ECU to the model and the real-time implementation, because sampling rates and I/O time delays play a crucial role in numerical stability as well as in the overall stability of the HIL simulation. Since the efficient parameterization and validation of such a model is essential for the HIL application process, the last section of the paper deals with model calibration and shows a comparison of measured and simulated in-cylinder values.

ENGINE MODEL REQUIREMENTS FOR ECU TEST SYSTEM

Nowadays, a wide range of mathematical approaches are used to simulate combustion engines. From simple mean value models to rather complex three dimensional fluid dynamic analyses, every approach is dedicated to its specific field of application. There is a big difference between complex models (e.g. GT-Power) and engine models for ECU development as proposed in this paper. The purpose of the complex models is the development and optimization of engines or just parts of them. The purpose of engine models as shown in this paper is to provide sensor signals for developing or testing ECUs. In this way expensive testbench hours could be partly replaced with less expensive HIL hours during ECU calibration [21].

Simulation models for engine ECU development and test application have to fulfill specific requirements. In a typical test environment the engine model is operated in closed-loop mode together with the ECU. The model has to generate consistent sensor values for all engine operation points (e.g. static and dynamic behavior, starting phase, engine cool-down, etc.) according to the applied actuator signals. The engine fault diagnostics should not detect any error during a closed loop simulation. For example, the cooling water temperature has to decrease after the engine has been switched off, as otherwise the ECU detects a malfunction of the temperature sensor. Another important requirement arises from real-time execution, which means that the calculation process has to be finished within the simulation step size. Closed loop simulation is not possible otherwise. Due to limitations, it seems obvious that very complex approaches will not be suitable for real-time simulation within the next few years. Thus, during the development of engine models for real time environments, the calculation load has to be kept in mind right from the beginning.

Models for engine development and ECU development do not compete with each other. On the contrary, they complement one another. To achieve completely virtual development, a complex engine model could be used to generate the test bench data of a new engine. This data set is then used to calibrate the engine model for the ECU development. Therefore, a simultaneous development of engine and ECU can be achieved.

A modular design permits the easy exchange or modification of parts of the model. This is an advantage if as a result of further development of the ECUs additional sensor signals are required. New ECU generations require the in-cylinder-pressure as an additional sensor signal. Engine models for developing and testing these ECUs therefore have to provide these signals.

Another important issue, especially in large test projects, is easy calibration of the simulation model. It must be possible to change between different engine variants very quickly. This imposes tough demands on the parameterization process, as it has to be possible to parameterize the simulation model with standard test bench measurement in a short time. Long feasibility studies and extensive parameter investigations are not practical for serial production projects with a limited time schedule and numerous different engine variants.

Another characteristic of engine models for ECU development is that they have to be usable offline on the PC and online in the real-time environment. The advantage is that the developer does not have to change the development environment, and only one model has to be parameterized.

INTRODUCTION TO MEAN VALUE ENGINE MODELS (MVEM)

For today's engine HIL-simulators MVEM are the standard approach [17][22][23][24][25]. Compared to in-cylinder models they are less complex but faster to calculate. For current HIL test system a MVEM can generate all necessary sensor signals and can incorporate all actuator signals in a way that a modern engine ECU will not detect any malfunction during closed loop operation. The next figure shows a connection diagram of a state of the art Diesel engine model [28] which can be used for a wide range of HIL simulation projects.

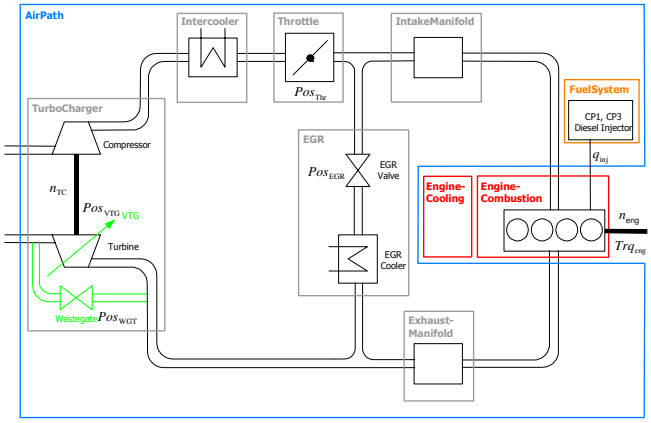

Figure 1: Structure of the MVEM

The components of the MVEM shown in figure 1 are:

- Intake manifold,
- Exhaust manifold,
- Throttle and intercooler,
- EGR valve and EGR cooler,
- Turbocharger,
- Fuel system and engine cooling system and
- Engine combustion.

Most of the governing equations for the different components have only minor differences between a MVEM and an in-cylinder model (e.g., fuel system, intake manifold, etc.). The two major differentiators can be found in the combustion model and in the cylinder filling model.

COMBUSTION SIMULATION

Instead of a crank-angle-based simulation, the concept for a MVEM uses the so-called mean indicated pressure. The definition of the mean indicated pressure can be seen in the following figure:

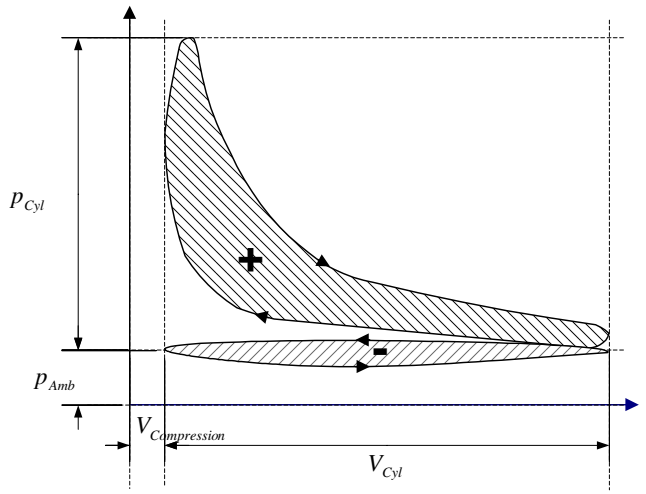

Figure 2: p-V diagram of an internal combustion engine

Figure 2 shows a typical p-V diagram for an internal combustion engine. The area marked with a plus sign can be seen as the high pressure cycle, the second area, marked with a minus sign, describes the gas exchange cycle. For a MVEM, these two areas are combined to form an equivalent rectangular area defined by cylinder displacement and mean indicated pressure.

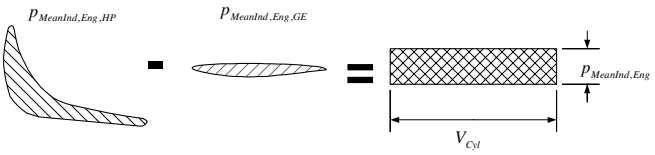

Figure 3: Definition of the mean indicated pessure

Under this assumption the thermodynamic cycle work of the engine can be calculated with the following equation:

$$W_{Cyl} = p_{MeanInd,Eng} V_{Cyl} \tag{1}$$

Dividing the cycle work by the time for one engine cycle the thermodynamic power for one cycle can be calculated:

$$P_{Cyl} = \frac{W_{Cyl}}{t_{Cycl}} = p_{MeanInd,Eng} V_{Cyl}\ i\ n_{Eng} = \frac{p_{MeanInd,Eng} V_{Cyl}}{t_{Cycl}}. \tag{2}$$

This thermodynamic power can be set equal to the mechanical power

$$P_{\mathrm{Cyl}} = Trq_{MeanInd,Eng}\ 2\,\pi\ n_{Eng}. \tag{3}$$

Finally, a relationship can be found between the internal mechanical and the thermodynamic torque with the following equation:

$$Trq_{MeanInd,Eng} = \frac{i\,V_{Cyl}}{2\pi}\, p_{MeanInd,Eng} \tag{4}$$

The indicated mean pressure can be calculated from an ordinary engine test bench measurement for every engine operation point. In the MVEM these values for different engine operation points are be stored in a map depending on the engine speed and the injected fuel mass. In order to incorporate further dependencies like the injection angle and the actual A/F value two efficiency functions stored in maps are multiplied with the mean indicated pressure. The different influences are described by the next equation:

$$p_{MeanInd,Eng,Cyl} = p_{MeanInd,Eng,Cyl,Ideal}\ (n_{Eng}, q_{Inj,Cyl}) \cdot \eta_{\lambda}(\lambda_{Cyl}) \cdot \eta_{Inj}(\varphi_{Inj,Cyl}) \tag{5}$$

The indicated mean pressure is retransformed to the indicated torque, and the effective mechanical torque is derived from it by subtracting the friction torque:

$$Trq_{MeanEff,Eng,Mod} = \sum_{Cyl} \frac{p_{MeanInd,Eng,Cyl,Mod} \cdot i \cdot V_{Cyl}}{2\pi} - Trq_{Fric}(n_{Eng}, T_{Eng}) \tag{6}$$

Finally, it can be stated that a MVEM is characterized by a set of equations transforming an ordinary engine test bench measurement into a table containing the mean indicated pressure. This value describes the combustion process for a complete cycle.

To simulate the engine torque production according to the crank angle, an ordinary mean value approach for the combustion process as discussed above is not sufficient. This approach calculates a combustion torque which remains constant over a complete engine cycle, thus no engine speed oscillations due to varying engine cycles are simulated. To overcome this drawback the mean value method has been extended by a so-called form function, which can be seen in the following figure.

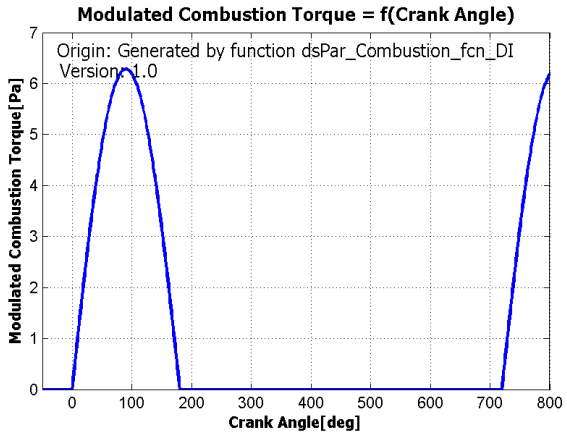

Figure 4: Form function over crank angle

The form function is positive during the combustion cycle and zero for the rest of the engine cycle. The mean indicated pressure is multiplied with this form function

$$p_{MeanInd,Eng,Cyl,Mod} = p_{MeanInd,Eng,Cyl} \cdot f(\varphi_{Crank,Cyl}) \cdot \qquad (7)$$

This function superimposes the crank angle effect onto the standard mean value approach. The form function is calculated from a sinus function as shown in figure 4.

AIRPATH

The air path simulates the compressor, intercooler, throttle and intake manifold dynamics on the intake side. On the exhaust side turbine, exhaust gas recirculation valve (EGR), cooler, and exhaust manifold are modeled.

The turbocharger is modeled as a compressor and turbine, connected to one another via the turbocharger shaft.

The intercooler cools the air flow from compressor according to the efficiency and temperature difference between input and coolant temperature. The throttle is modeled as an orifice with a variable cross-section which limits the fresh air flow into the intake manifold.

The mass of gas in the intake manifold is calculated from mass flow balance and the temperature of the manifold from energy balance. The pressure follows from the ideal gas equation.

The same simulation approach is used for the exhaust manifold. In difference to the throttle the mixing of fresh air with exhaust is calculated.

The EGR cooler cools the air flow from combustion depending on efficiency and temperature difference between input and coolant temperature. The EGR is simulated as a valve. The EGR position can increase the air flow into the intake manifold.

The different models can be categorized as three general subcomponent models:

- Accumulator,
- Valve and
- Cooler

These three approaches are discussed in the next chapters. Finally, the implementation of the turbocharger and the filling of the cylinder will be discussed.

Accumulator

The accumulator is modeled as a thermodynamic control volume using mass- and energy balances for three components i = {air, fuel and exhaust}.

$$\frac{dm_{i,Acc}}{dt} = \dot{m}_{i,Acc,In} - \dot{m}_{i,Acc,Out} \qquad (8)$$

$$dU_{Acc} = dW_{Acc} + dQ_{Acc} + dH_{Acc} \qquad (9)$$

The next figure shows the input and output values.

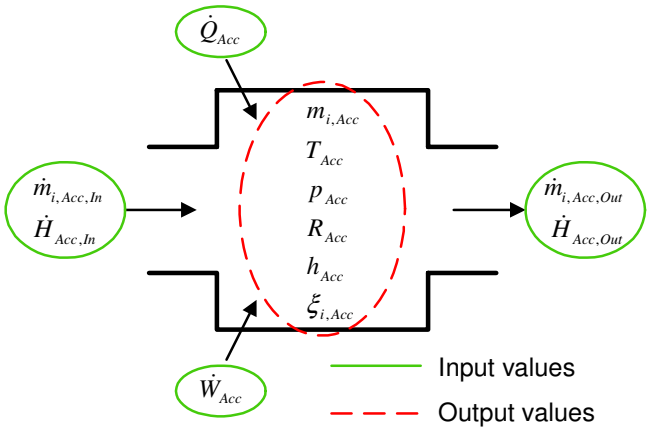

Figure 5: Input and output values of the accumulator calculation

Depending on the mass fraction for each component, the model calculates the gas constant R_{Acc}, the specific heat capacity c_v, the specific internal energy u and the specific enthalpy h.

A differential equation for the accumulator temperature can be derived from the energy balance:

$$dT_{Acc} = \frac{dW_{Acc} + dQ_{Acc} + dH_{Acc} - \sum_i dm_{i,Acc} u_i}{m_{Acc} c_{v,Acc}} \qquad (10)$$

The four parts in the numerator of this equation describe:

- The work due to volume change dW_{Acc},
- The heat release and wall heat flow dQ_{Acc},
- The enthalpy flow over the control volume boundary dH_{Acc}

- A term from the definition of the internal energy $\sum_i dm_{i,Acc} u_i$ for every gas component.

The accumulator pressure is calculated by the ideal gas law, assuming ideal gas behavior.

$$p_{Acc} = \frac{m_{Acc} R_{Acc} T_{Acc}}{V_{Acc}} \tag{11}$$

The equations discussed above are used for simulating the intake and exhaust manifold in the MVEM as well as for describing the combustion chamber in the in-cylinder model.

Valves

This chapter introduces the general concept of a valve which was used for modeling the throttle and EGR valve in the MVEM. For the in-cylinder model, the concept was also applied to the intake and exhaust valve model. The following schematic shows a universal orifice with the input and output values and the calculated mass and enthalpy flows.

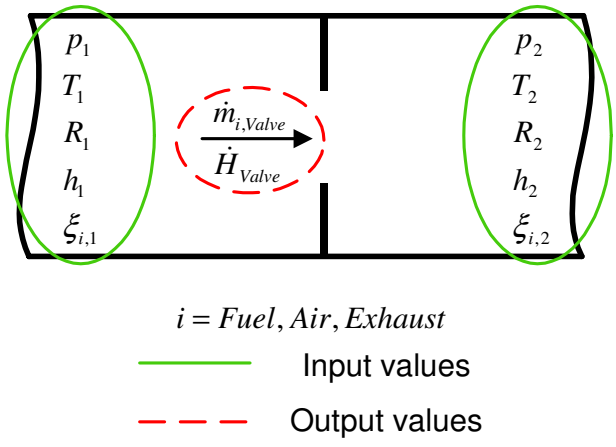

Figure 6: Input and output values of the valve calculation

We are assuming an isentropic, adiabatic flow through the orifice as the basis for calculating the mass flow.

$$\dot{m}_{Valve} = A_{Valve} \frac{p_i}{\sqrt{R_i T_i}} \Psi\left(\frac{p_2}{p_1}, \kappa_i\right) \tag{12}$$

It has to be considered that every valve has a certain flow direction defining which values have to be used as input for calculating the output values.

The definition of the flow function Ψ can be seen in equation (13). Note that the flow function has a maximum value at the critical pressure ratio described by $\frac{p_2}{p_1} = \left(\frac{2}{\kappa+1}\right)^{\frac{\kappa}{\kappa-1}}$. Beyond this pressure ratio, the mass flow reaches the speed of sound, which cannot be increased in an ordinary orifice. The different cases for the two flow directions are summarized in the following equation.

$$\Psi\left(\frac{p_2}{p_1}, \kappa\right) = \begin{cases} \left(\frac{2}{\kappa+1}\right)^{\frac{1}{\kappa-1}} \sqrt{\frac{2\kappa}{\kappa+1}} & , \; 0 < \frac{p_2}{p_1} < \left(\frac{2}{\kappa+1}\right)^{\frac{\kappa}{\kappa-1}} \\ \sqrt{\frac{2\kappa}{\kappa-1}\left[\left(\frac{p_2}{p_1}\right)^{2/\kappa} - \left(\frac{p_2}{p_1}\right)^{\frac{\kappa+1}{\kappa}}\right]} & , \; \left(\frac{2}{\kappa+1}\right)^{\frac{\kappa}{\kappa-1}} \le \frac{p_2}{p_1} < 1 \\ -\sqrt{\frac{2\kappa}{\kappa-1}\left[\left(\frac{p_1}{p_2}\right)^{2/\kappa} - \left(\frac{p_1}{p_2}\right)^{\frac{\kappa+1}{\kappa}}\right]} & , \; 1 \le \frac{p_2}{p_1} < \left(\frac{2}{\kappa+1}\right)^{-\frac{\kappa}{\kappa-1}} \\ -\left(\frac{2}{\kappa+1}\right)^{\frac{1}{\kappa-1}} \sqrt{\frac{2\kappa}{\kappa+1}} & , \; \left(\frac{2}{\kappa+1}\right)^{-\frac{\kappa}{\kappa-1}} \le \frac{p_2}{p_1} \end{cases} \tag{13}$$

Figure 7 shows the flow function for different isentropic coefficients.

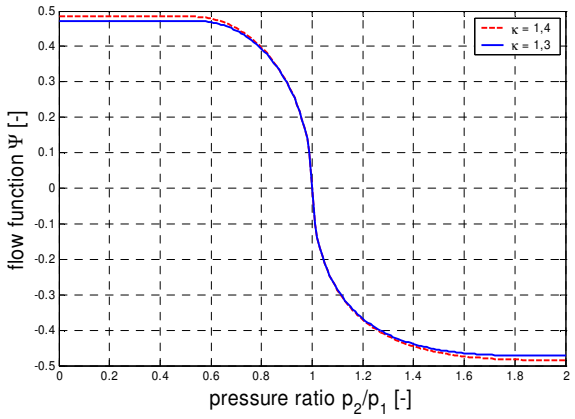

Figure 7: Flow function

It can be seen that differences between isentropic constants play a minor role in calculating the flow function. A fixed isentropic coefficient was therefore chosen. The mass flow of the individual components can be calculated from the individual mass fractions:

$$\dot{m}_{i,Valve} = \dot{m}_{Valve} \xi_{i,Valve} \tag{14}$$

The enthalpy flow can be calculated with the following equation:

$$\dot{H}_{Valve} = \dot{m}_{Valve} h_{Valve} \tag{15}$$

Cooler

The cooler is modeled using an efficiency which is calculated from the engine test bench measurement:

$$\eta_{Cooler} = \frac{T_{In,Cooler} - T_{Out,Cooler}}{T_{In,Cooler} - T_{Coolant}} \tag{16}$$

The efficiencies for the engine operation points are stored in a table according to engine speed and injected fuel mass.

Cylinder filling

In a MVEM, the cylinder filling of the engine can be modeled by the idea of a piston pump, using the following equation:

$$\dot{m}_{Valve,Ideal} = i\, n_{Eng}\, V_{Cyl}\, \rho_{IntMan} \tag{17}$$

Due to the nonideal behavior of a real engine, a volumetric efficiency coefficient has to be introduced in order to incorporate real cylinder mass flow behavior into the piston pump equation for all engine operation points. The volumetric efficiency is defined by the following equation:

$$\eta_{vol}(n_{Eng}, p_{InMan}) = \frac{\dot{m}_{Valve,Measurement}}{\dot{m}_{Valve,Ideal}} \tag{18}$$

Using this definition, a map of the volumetric efficiency for all engine operation points can be prepared during model parameterization. The mass flow into the cylinder can be calculated very accurately for all engine operation points from this table in combination with the equation for an ideal piston pump.

Turbocharger

Turbochargers are used to compress the air flowing into the engine. This increases the amount of air in the cylinder per cycle. The turbocharger model is separated into three main parts:

- Compressor,
- Shaft and
- Turbine.

The following figure shows the components and their input and output variables.

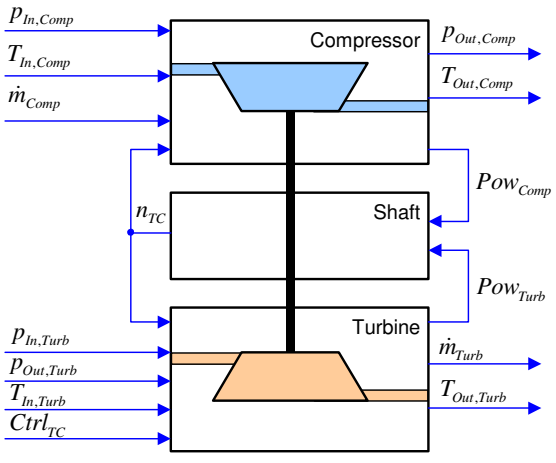

Figure 8: Structure of the turbocharger model

Compressor and turbine are coupled by a power balance calculating the turbocharger shaft speed

$$\dot{n}_{TC} = \frac{1}{J_{TC}}\left(\frac{P_{Comp}}{n_{TC}} + \frac{P_{Turb}}{n_{TC}}\right) \tag{19}$$

The compressor and turbine power are defined by the following equations

$$P_{Turb} = \dot{m}_{Turb} c_{p,air} \eta_{Turb,is} T_{In,Turb}\left(1 - \left(\frac{1}{\Pi_{Turb}}\right)^{\frac{\kappa-1}{\kappa}}\right) \tag{20}$$

$$P_{Comp} = \dot{m}_{Comp} c_{p,air} \frac{1}{\eta_{Comp,is}} T_{In,Comp} \left(\Pi_{Comp}^{\frac{\kappa-1}{\kappa}} - 1\right) \tag{21}$$

The turbine mass flow and efficiency are contained in maps. The turbine pressure ratio is calculated from the exhaust manifold pressure and the ambient pressure.

$$\dot{m}_{Turb,red} = Map(\Pi_{Turb}, Ctrl_{TC}) \tag{22}$$

$$\eta_{Turb} = Map(\dot{m}_{Turb,red}, n_{TC,red}) \tag{23}$$

The compression ratio and efficiency for the compressor are stored in maps. The mass flow is calculated externally by the throttle valve.

$$\Pi_{Comp} = Map(\dot{m}_{Comp,red}, n_{TC,red}) \tag{24}$$

$$\eta_{Comp} = Map(\dot{m}_{Comp,red}, n_{TC,red}) \tag{25}$$

The maps are parameterized with steady-state measurement data supplied by the manufacturer.

Finally, the compressor model calculates the boost pressure, and the turbine model the exhaust mass flow. The turbine mass flow can be controlled either by a variable turbine geometry input or by a wastegate valve.

INTRODUCTION TO CRANK ANGLE BASED ENGINE MODELS

In-cylinder models are more physically based than MVEMs. Parameterization is therefore more complex, but extrapolation is easier, for example, the variable valve timing which is also used to reduce emissions in diesel engines [1]. With a MVEM, the effect of the variable valve timing can only be simulated by multiple volumetric efficiency maps that require a lot of test bench measurements. In an in-cylinder model, only the relationship between camshaft position and valve lift has to be adapted. In-cylinder models also provide the in-cylinder

pressure signal that is needed for future engine management concepts [2][3][15]. Several simulations products are already available incorporating some of the presented ideas and equations [38][39][40].

NEW MODEL PARTS

The in-cylinder model (Figure 9) is based on the MVEM.

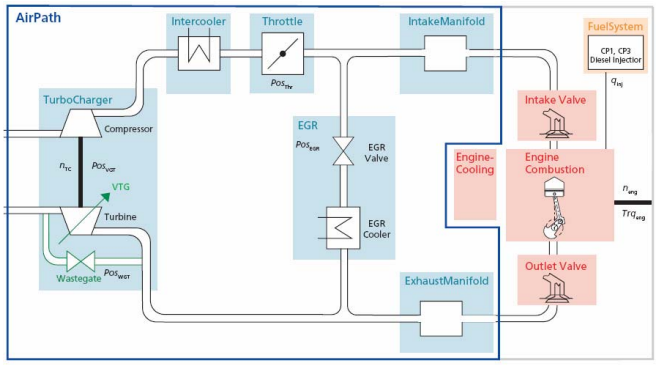

Figure 9: Structure of the in-cylinder model

The new model parts are:

- Intake and exhaust valves and
- Combustion chamber with crankshaft dynamics.

The fuel system of the MVEM also has to be adjusted. It consists of:

- Rail
- High-pressure pump
- Pressure control valve
- Injector

The injector has to be modified for the in-cylinder model. The other modules can be taken from the MVEM.

SET UP OF THE DIFFERENTIAL EQUATIONS

There are two ways to set up the differential equations of an engine model: time based and crank angle based. One advantage of an angle-based equation setup is that the heat release approaches described in the literature are almost all crank angle based. The objective of obtaining the output of the engine model with a fixed crank angle step size is also important. The following equation gives the relationship between the time step size and the crank angle step size.

$$d\varphi = \omega \, dt \tag{26}$$

However, a crank angle based engine model has one major drawback. At low engine speed the fixed crank step size involves a large time step size. This results in numerical instability. The extreme case is an engine at standstill which cannot be simulated with a crank angle based model. Yet this case is essential for simulating the starting, stopping and cooling down of the engine. All equations are converted to time-based differential equations.

INTAKE AND EXHAUST VALVES

The modeling of the intake and exhaust valves is based on the universal valve described in the MVEM chapter. The specific of the intake and exhaust valves is the calculation of the cross-section area in equation (27) derived from (12). It is computed from a reference area in the valve channel and the flow coefficient μ according to [18].

$$\dot{m}_{InValve} = A_{InValve}\,\mu(l_{Valve})\,\frac{p_{InValve}}{\sqrt{R_{InValve}\,T_{InValve}}}\,\Psi\left(\frac{p_{Cylinder}}{p_{InMan}}, \kappa_{InValve}\right) \tag{27}$$

The flow coefficient depends on the valve lift and the flow direction (Figure 10). Because of the awkward geometry, the spilling out is worse than the pouring in. Valve timing can be easily simulated by changing the relation between camshaft position and valve lift variable. Since the valve can be passed through bidirectionally, the internal exhaust gas recirculation is modeled correctly.

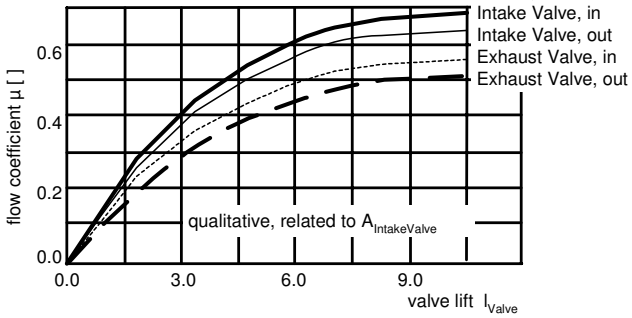

Figure 10: Flow coefficient

COMBUSTION CHAMBER

The model of the combustion chamber is based on the accumulator equations. Some extensions have to be introduced to the equations compared to the intake and exhaust manifold.

Mass Balance

In the mass balance, the combustion reduces the air and fuel mass and increases the exhaust mass. The injected fuel mass flow also has to be considered:

$$\frac{dm_{i,Cyl}}{dt} = \dot{m}_{i,IntakeValve} + \dot{m}_{i,Inj} \pm \dot{m}_{i,Burned} - \dot{m}_{i,ExhaustValve} \tag{28}$$

Since the mass calculation for every component (fuel, air, exhaust) is done separately and based on continuous integration of the mass flow, the residual exhaust gas is automatically taken into account.

Energy Balance

The temperature in the combustion chamber is calculated in equation (10).

$$dT_{Cyl} = \frac{1}{m_{Cyl} c_{v,Cyl}} \left(dW_{Cyl} - dQ_{Wall,Cyl} + dQ_{Fuel} + dH_{IntakeValve} + dH_{Inj} - dH_{ExhaustValve} - \sum_i dm_{i,Cyl} u_{i,Cyl} \right) \quad (29)$$

The different energy flows taken into account are also shown in Figure 11.

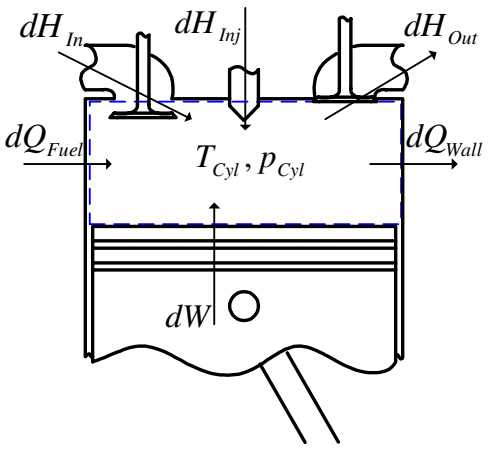

Figure 11: Energy flows into and out of the combustion chamber

For the wall heat, the well known approach from Woschni [5] is applied. For the heat release different approaches are analyzed below.

HEAT RELEASE FUNCTIONS

Real combustion is a very complex process. Even three-dimensional computational fluid dynamics (CFD) approaches describe it only approximately. These models are inappropriate for real-time-applications due to the enormous computing time. In order to simulate the correct in-cylinder pressure and temperature, it is important to use a suitable type of heat release function. Four different approaches to calculating the rate of heat release (ROHR) that can be considered for real-time-applications are discussed below.

Shape Functions

A still very popular approach is shown in [6]. This is only the most familiar example of a whole group, the shape functions. There are many variants as double-Vibe and multiple-Vibe. The polygon and hyperbole approaches also belong to this group. The shape function determines the distribution of the heat release versus crank angle. According to [6] the heat release is calculated from:

$$\frac{dQ_{Fuel}}{dt} = m_{Fuel,total} Q_{LHV} \dot{\varphi} \frac{C(m_v + 1)}{\Delta\varphi_{CD}} \left(\frac{\varphi - \varphi_{CS}}{\Delta\varphi_{CD}} \right)^{m_v} e^{-C\left(\frac{\varphi - \varphi_{CS}}{\Delta\varphi_{CD}} \right)^{m_v+1}} . \quad (30)$$

The shape function can be adapted to different engine operating points with three parameters m_v, $\Delta\varphi_{CD}$ and φ_{CS}. In [7] it is shown how the parameter can be extrapolated for any operating point from a reference operating point. Different ignition delay times are taken into account by adjusting φ_{CS}. A possible method of automatic calibration with measurement data is provided in [8].

Arrhenius-approach

In [9] it is proposed calculating the heat release with the approach of Arrhenius. It is based on the fuel concentration. According to Arrhenius the reaction rate depends on the temperature:

$$k_R = A e^{-\frac{E_A}{RT}} . \quad (31)$$

This reaction rate is applied to the fuel combustion:

$$C_x H_y + \left(x + \frac{y}{4} \right) O_2 \longrightarrow x CO_2 + \frac{y}{2} H_2 O \quad (32)$$

The change in CO_2 concentration is calculated from:

$$\frac{dC_{CO_2}}{dt} = A e^{-\frac{4650}{T}} C_{O_2} C_{C_x H_y} \quad (33)$$

And the heat release results from:

$$\frac{dQ_{Fuel}}{dt} = \frac{dC_{CO_2}}{dt} \frac{1}{x} m_{Cyl} Q_{LHV} \quad (34)$$

The Arrhenius parameter k_R is regarded as dependent on the engine operation point to calibrate the model. Philipp [9] specifies the ignition delay time by

$$t_{ID} = 4{,}4e-4 \left(\frac{p_{Cyl}}{10^5} \right)^{1{,}02} e^{\frac{4650}{T_{cyl}}} . \quad (35)$$

Mixing Controlled Combustion (MCC) [10]

Another approach to predicting the heat release assumes mixing controlled combustion. This phenomenological model is based on the injection rate and the fuel concentration in the combustion chamber.

Chmela [10] applies the k-ε theory from Magnussen [11] in a zero-dimensional combustion model. The result is a combustion model based on the idea that the injection-spray jets produce turbulent energy. This turbulent energy is the dominant effect for the time behavior of the fuel reaction. The kinetic energy has to be introduced in advance of calculating the turbulent energy. The kinetic energy introduced by the injected fuel mass therefore has to be calculated:

$$\frac{dE_{kin,Fuel}}{dt} = \frac{1}{2}\rho_{Fuel}\left(\frac{1}{\mu A_{Inj}}\right)^2\left(\frac{dV_{Fuel,Inj}}{dt}\right)^3 \tag{36}$$

Afterwards the kinetic energy in the cylinder can be derived from the injected and the dissipated kinetic energy:

$$\frac{dE_{kin,Fuel,Diss}}{dt} = \frac{dE_{kin,Fuel}}{dt} - c_{Diss}E_{kin,Fuel,Diss} \tag{37}$$

To calculate the turbulent energy density k, the kinetic energy is related to the total mass participating in the combustion process.

$$k = c_{Turb}\frac{E_{kin,Fuel,Diss}}{m_{Fuel,Inj}(1+\lambda_{Diff}L_{St})} \tag{38}$$

The heat release is computed by:

$$\frac{dQ_{Fuel}}{dt} = c_{Mod}\,m_{Fuel}\,e^{c_{Rate}\frac{\sqrt{k}}{\sqrt[3]{V_{Cyl}}}}. \tag{39}$$

This approach does not take ignition delay into account. Lakshinarayanan et al. [12] state that higher temperature at the beginning of injection by an increased compress ratio reduced the delay period so substantially that the delay could be ignored.

Evaporate Controlled Combustion [13]

Constien [13] shows an evaporate controlled heat release approach. The injected fuel mass is divided into mass fractions per simulation step size t_k by:

$$m_{Fuel,Inj}(t_k) = \rho_{Fuel}\int_{t_k}^{t_{k+1}}\frac{dV_{Fuel,Inj}}{dt}dt\,. \tag{40}$$

It is assumed that all drops of the injected fuel mass have the Sauter mean diameter defined by the following relation:

$$d_s(t_k) = 8{,}7e^{-6}d_N(Re\,We)^{-0.28}\,. \tag{41}$$

Where the Reynold number and the Weber number are defined as:

$$Re = \frac{v_{Fuel,Inj}d_N}{\nu_{Fuel}} \tag{42}$$

$$We = \frac{{v_{Fuel}}^2 d_N \rho_{Cyl}}{\sigma_{Fuel}} \tag{43}$$

The number of droplets is calculated from the fuel quantity and the droplet diameter derived from the mass fraction per simulation step size:

$$n_{Tr}(t_k) = \frac{m_{Fuel,Inj}(t_k)}{\frac{\pi}{6}d_s(t_k)^3\rho_{Fuel}} \tag{44}$$

These calculations are made for the currently injected fuel mass $m_{Fuel,Inj}(t_k)$ in every step. The number of drops of a portion is fixed, only the drop diameter decreases due to evaporation. The following calculations have to be done separately for every injected fuel portion (index m) in every time step (index k). The surface of the portion is give by:

$$A_{Tr,m}(t_k) = n_{Tr}(t_m)\pi d_{s,m}^2(t_k) \tag{45}$$

The vaporized fuel mass depends on this surface, the cylinder pressure and the current drop diameter:

$$m_{evap,m}(t_k) = C_{Diff}A_{Tr,m}(t_k)\,p_{Cyl}(t_k)^{m_p}\frac{1}{d_{s,m}(t_k)} \tag{46}$$

Consequently the fuel mass of the drops decreases.

$$m_{Fuel,Inj,m}(t_k) = m_{Fuel,Inj,m}(t_{k-1}) - m_{evap,m}(t_k) \tag{47}$$

The new drop diameter is computed from:

$$d_{s,m}(t_k) = \sqrt[3]{\frac{m_{Fuel,Inj,m}(t_k)}{\frac{\pi}{6}n_{Tr}(t_m)\rho_{Fuel}}}\,. \tag{48}$$

The ignition delay is calculated according to [14]:

$$t_{ID} = a\left(\frac{p_{Cyl,mean}}{10^5}\right)^b e^{\frac{c}{T_{cyl,mean}}} \quad (49)$$

For each evaporated fuel portion, the simulation model calculates whether the time difference between the actual simulation time and the time at which the individual fuel portion was injected is smaller than the actual ignition delay. In this case the portion is completely burned. The heat release can be calculated from:

$$\frac{dQ_{Fuel}}{dt} = Q_{LHV}\sum_{m=1}^{k} m_{Fuel,Burned,m}(t_k) \quad (50)$$

Injection capture with HIL Simulators

For closed–loop-testing of an ECU, its injection signals have to be taken in account in the engine model. In general there are two ways of capturing the injection signals from an ECU at an HIL test bench. These are the window-based and the continuous injection signal measurement [30], [29].

Window-based injection measurement is shown in Figure 12. The rising edges and the durations of the injection signal are captured in a predefined event capture window. At the end of the event capture window, the new measurement data is provided to the model. The injection quantity is computed from the duration of the injection pulses by means of a map. The output is the total injected fuel quantity, which is needed for the MVEM or the shape functions.

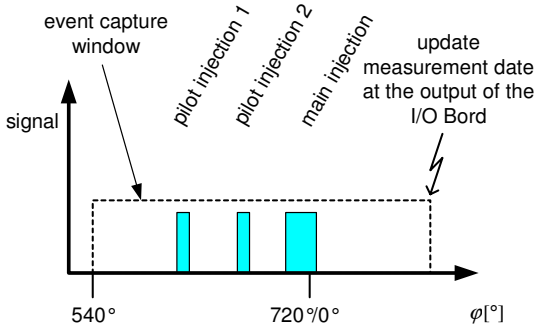

Figure 12: Window-based injectiion capture

Figure 13 shows continuous injection capture. The state and the value are read from the I/O board in each time step. While the injection signal lasts the state is “1” and the value returns the position of the rising edge. Otherwise the state is “0” and the value returns the duration of the last injection signal. The fuel flow into the combustion chamber is calculated from these signals. Only standard ECU parameters are needed for parameterizing this model part. Continuous injection capture is the appropriate method for heat release calculation according to Arrhenius, Chmela, and Constien.

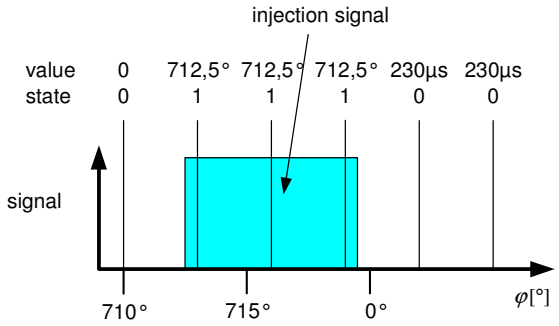

Figure 13: Continuous injection capture

Qualification for the HIL-application

In general, shape functions offer the advantage of approximating every ROHR by using different shape function variants. They also involve low computation effort. The model input variable is the total injected fuel quantity per cycle, which is a possible reason for implementation problems, especially in real-time simulation environments. The measurement of the total injected fuel mass of the current cycle cannot be completed before the combustion process itself begins (Figure 14). Using the injected mass of the previous cycle cannot solve this problem because the idle speed control will become unstable due to the delay of a complete engine cycle. Thus, shape functions are inappropriate for HIL simulations of diesel engines.

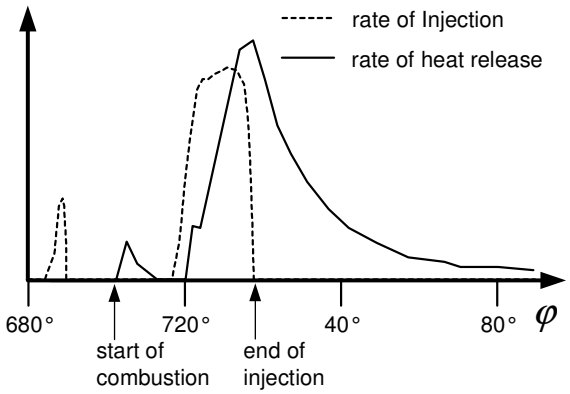

Figure 14: Typical rate of injection and rate of heat release

The Arrhenius approach is based on the fuel concentration in the combustion chamber. The literature [6] states that the Arrhenius approach is basically only applicable to bimolecular reactions. However, diesel combustion is a typical chain reaction. To overcome this apparent drawback, the Arrhenius parameter is calculated according to operating point. Because there is only a single parameter, the adaptation possibilities are limited.

The approach from Chmela [10] is based on fuel concentration and turbulent energy density in the combustion chamber. It offers three independent parameters and in this regard more possibilities for adaptation to test bench data. Bargende [15] shows that it might be impossible to find appropriate parameters that are applicable to all en-

gine operating points. The parameters must therefore be considered operating-point-dependent.

The literature includes several modifications. Lakshinarayanan et al. [12] expands the model in such a way that the impact of spray on the wall can be considered. Pirker [20] and Barba [15] discuss modifications that take partly premixed combustion into account.

Constiens [13] model is based on evaporation. Because fuel mass is discretized in portions, the computation effort is higher. However, it is possible to use this approach for real-time simulation [16].

The shape functions are inappropriate for HIL simulation. The computation effort of Constiens approach [13] is problematic for real-time applications. The Chmela [10] and the Arrhenius approaches are therefore analyzed and compared with test bench data. According to Lakshinarayanan et al. [12] the ignition delay is also neglected in the Arrhenius approach.

REAL-TIME IMPLEMENTATION

The model equations were implemented with MATLAB®/Simulink® from The MathWorks. As a basis for implementing the in-cylinder models, the MVEM diesel engine simulation package from dSPACE's product family Automotive Simulation Models (ASM) was used. The package is an open Simulink model for the real-time simulation of turbocharged diesel engines and is specially designed for the hardware-in-the-loop testing of ECUs – as well as for the controller design phase. Since the diesel engine simulation package is an open Simulink model, additional components can be added and existing models can be replaced very easily. Existing engine components like turbocharger, throttles, etc., and also models for longitudinal drivetrain and environment devices (e.g. driver models), ensure a good starting point for developing more sophisticated models as presented in this paper.

Mean value Diesel engine models as discussed in the first section of this paper (e.g., with 6 cylinders, EGR, turbocharger, common-rail injection system and diverse auxiliary models) can be executed on a state-of-the-art HIL system (e.g. dSPACE DS1006, 2.6 GHz) with a sample rate of 1 ms and simple Euler integration. The execution time is about 65 µs, i.e. only a 6.5 % processor load.

Due to numerical reasons even for MVEMs a sample rate of 1 ms is often not sufficient for a numerical stable integration of the mass flow through the engine. Especially for smaller manifold volumes the models gets a stiff behaviour. Therefore an oversampling of these parts has been implemented by using a "for-iterator" subsystem and a special integration block. With about ten intermediate integration steps typical systems can be handled.

For a 4-cylinder crank-based engine model, it is useful to separate the auxiliary model components from the core engine model because the core model needs a higher sample rate for numerically stable integration and to get a sufficient cylinder pressure resolution. Due to the small step size and the complex model, the model implementation must be optimized to reduce the computation effort. A deliberate model structure helps to avoid duplicate computations. Trigonometric functions and power functions have been avoided because they take huge computation effort. Sampling the engine model at a rate of 100 µs, while the auxiliary models just run at 1 ms provides the cylinder pressure with a resolution of 0.6° or 3.6° crank angle for 1000 rpm and 6000 rpm respectively. On a 2.6 GHz DS1006 real-time processor board, the execution time of the 100 µs-task is about 55 µs. Including the auxiliary models this leads to a total processor load of about 70 %.

Using specialized I/O hardware, it is also possible to integrate the model on a "pseudo" crank-angle basis. Using a crank-angle equidistant HW-interrupt, the model evaluation is done with a constant crank angle step size (e.g. one or two degrees). The time-based differential equations are implemented in Simulink (HW-triggered) subsystem which uses a special variable time step integrator. The actual time step of the integrator is calculated by dividing the constant crank angle step by the engine speed for each integration step. For high ($\gtrsim$ 4000 rpm) and low ($\lesssim$ 1700 rpm) engine speeds, this approach results in very small (not real-time capable) or very big (numerically unstable) equivalent integration "time" steps. Therefore, a mechanism has to be established to switch back to constant time-step integration in these operating phases. Since this effort is normally not justified by the benefits of the crank-based integration scheme the majority models today use a constant time based integration.

Since ECUs using in-cylinder pressure sensors, typically calculate the MFB50 (50% mass fraction burned) as a "mean" value for control purposes, the above mentioned crank angle resolution should be sufficient. If a higher resolution is required, e.g., because a precise peak pressure has to be simulated, the model can be run on two real-time processors to speed up the calculation.

Since today, a 6-cylinder in-cylinder model was successfully tested in closed-loop operation on an HIL system with a mass production ECU, a BOSCH EDC 16

MODEL CALIBRATION

For the MVEM, a standard parameterization process is available and established in numerous HIL projects. At the beginning of an HIL project, a set of parameters and test bench measurements is gathered from the customer. Some parameters can be used directly without further calculation (e.g., number of cylinders, engine displacement, etc.), other parameters need to be calculated from the test bench measurements, e.g., the mean indicated pressure. Finally, a set of parameters characterizing the simulation model is produced in such a way that the test bench measurements can be reproduced. The

process itself is straightforward, which means that model parameter can be calculated by input data without an optimization loop.

This widely accepted approach has to be extended for in-cylinder models. Many parameters can be calculated in the same way as for the MVEM, but an extended parameterization process is necessary for the filling and empting of the cylinder and for the combustion process itself. It seems obvious that the well-known, straightforward approach established for the MVEM is not transferable to the parameterization of in-cylinder models. Due to the transient model behavior, a parameterization process for in-cylinder models will rely on a combination of simulation and parameter optimization.

The next figure presents a brief sketch of such a process. The following ideas rely mainly on the investigations presented in [19].

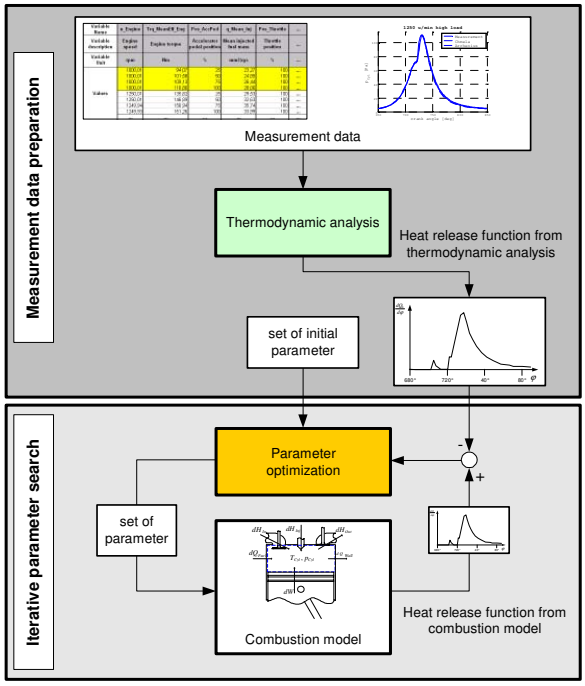

Figure 15: Parameterization process

In principal the process can be divided into two separated steps

- Measurement data preparation and
- Iterative parameter search.

The first step of this process, measurement data preparation, aims to calculate a heat release function from the in-cylinder pressure measurement and standard engine test bench measurement data. With this initial step the integral value cylinder pressure including the wall heat flux, the work due to volume change and the enthalpy flow from the different input and output masses could be reduced to the heat release function. After transforming the pressure measurements to a heat release curve the second step of the parameterization process - iterative parameter search - can be initiated. With a set of initial parameters for a specific combustion model an optimization algorithm starts to simulate the combustion process. As a result a heat release curve is generated. Comparing this simulated heat release with the one from the thermodynamic analysis a characteristic error (e.g. least square error) can be calculated feeding as input value for the optimization process. Therefore, the automatic process generates combustion function parameter for all engine operating points.

The presented parameterization process is currently under development. It seems obvious that without such a process the parameterization effort for in-cylinder models will be very time consuming. Today's HIL projects with its numerous engine variants are often characterized by a tough time schedule. With today's MVEM a nearly automated parameterization is already available. Since in-cylinder models require more effort for model calibration, also here, an automated process as presented is mandatory for the prosperity and acceptance of in-cylinder models in real-time applications and engine controller test systems.

SIMULATION RESULTS

For the simulation of the in-cylinder pressure, it is important that the peak pressure value and peak pressure position correspond as closely as possible to the measurement data. In addition, the engine power should agree.

Table 1 below compares simulation results for the in-cylinder pressure with the Chmela and Arrhenius approaches with measurement data at four different engine operation points. The four combustion parameters of the Chmela approach and the single one of the Arrhenius parameter were optimized for each engine operation point. Further, the wall temperature is adjusted for every engine operation point. This is necessary because only with the correct wall heat loss a correct in-cylinder pressure can be simulated, especially in the compression phase. The optimum parameter value of the wall temperature, which results in a minimum deviation between measured and simulated in-cylinder pressure, is different for the Chmela and the Arrhenius approach. A more detailed analysis yields that the variation of the parameter is smaller in the Chemla approach than in the approach based on Arrhenius. For initial rough calibration of the model, it would appear possible to regard them as constants. The Arrhenius parameter varied over a wide range. Examinations with different engines have to show to what extent the calibration for one engine can be reused for another.

Table 1: Parameters of ROHR models at different setpoints

Chmela:				
	1250rpm low load	1250rpm high load	3000rpm low load	3000rpm high load
c_{Diss}	0.1	0.1	0.1	0.1
c_{Turb}	0.2	0.2	0.2	0.2
c_{Rate}	0.0009	0.00115	0.0009	0.0014
c_{mod}	12.0 e9	15.5 e9	13.0 e9	14.5e9
T_{Wall}	500 K	670 K	600 K	880 K
Arrhenius				
	1250rpm low load	1250rpm high load	3000rpm low load	3000rpm high load
K_{Arrh}	14.8 e6	2.85 e6	6.7 e6	2.6 e6
T_{Wall}	420 K	800 K	600 K	880 K

Figure 16 shows the comparison of the in-cylinder pressure characteristic at low engine speed and low load. Though it is obvious that at this operation point the ignition delay cannot be neglected, the peak pressure is almost simulated correctly.

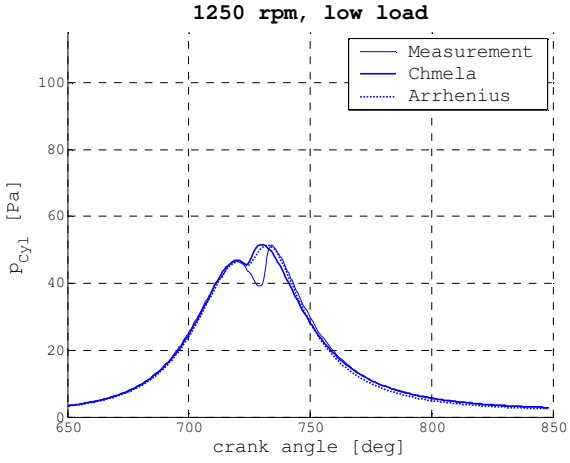

Figure 16: Comparison at low load and low speed

The comparison in Figure 17, at low speed and high load, shows that simulation results for peak pressure agree well with the measurement. The effect of the ignition delay is still visible but can be neglected. In the expansion phase, the simulated pressures are too low. This effect is greater with the Arrhenius approach than with the Chmela approach.

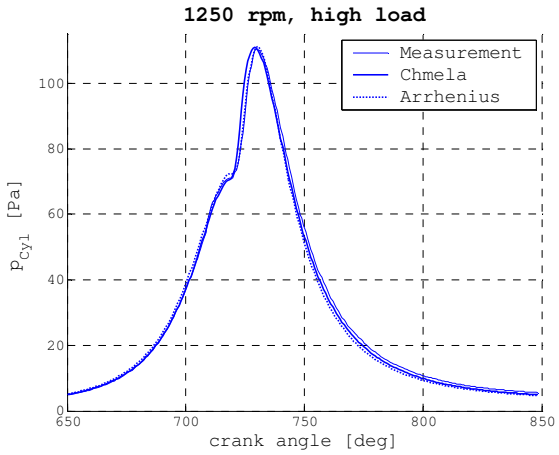

Figure 17: Comparison at high load and low speed

Figure 18 shows the comparison at low load and high speed. Both approaches show deviations in the simulated peak pressure. At this operation point the ignition delay has to be taken into consideration. Again, the Arrhenius approach simulated too-low pressures in the expansion.

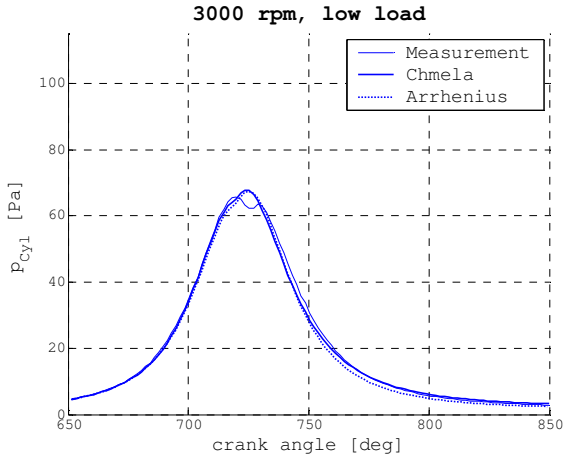

Figure 18: Comparison at low load and high speed

At high load and high speed (Figure 19), the simulated peak pressure agrees with the measurement. However, in the expansion phase the simulated pressure is again too low, especially with the Arrhenius approach.

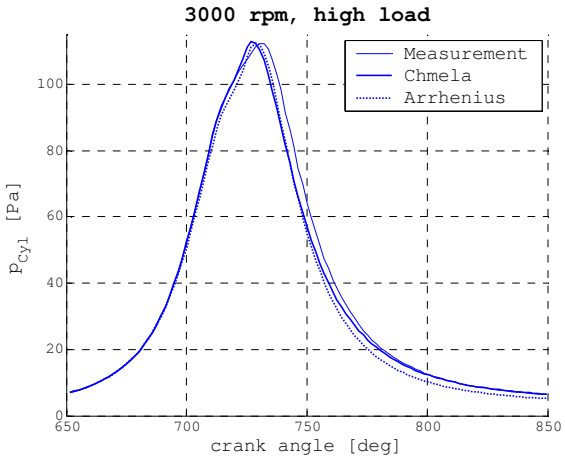

Figure 19: Comparison at high load and high speed

The simulated and measured engine power is given in Table 2.

Table 2: Comparison of the power

	1250rpm low load	1250rpm high load	3000rpm low load	3000rpm high load
Measured	9.3 kW	23.5 kW	15 kW	56.4 kW
Chmela	9.0 kW	21.2 kW	16 kW	48.3 kW
Arrhenius	8.3 kW	19.0 kW	10.0 kW	41.1 kW

The Arrhenius approach tends to result in a too-low engine power. This is a result of the too-low in-cylinder pressure in the expansion. As a result of the piston kinematics, the pressure in the area of top dead center has only a small effect on the generated power. The pressure 90° after top dead center has the greatest effect.

The impact of the Arrhenius parameter on the expansion pressure is low compared to the influence on the peak pressure. Thus, a better approximation of the generated engine power results in a worse approximation of the peak pressure. During the development phase and the investigations for the modeling approaches presented in this paper, it seems to be difficult to rely on the generated engine power for calibrating the Arrhenius model [9].

The peak pressure and the peak pressure position can be correctly simulated with both approaches. With the Arrhenius approach it is more difficult to generate the appropriate engine power. To simulate the correct in-cylinder characteristic, the model must be enhanced by taking the ignition delay into regard.

CONCLUSION AND OUTLOOK

Due to the continuously growing demand on pollutant exhaust gas reduction and the steadily growing pressure to improve engine fuel consumption a further refinement of engine and electronic engine (combustion) controller can certainly be expected in the future. In parallel the enabling technologies like improved micromechanics, sensor technology and higher processing power at reasonable cost, will lead to new demands on the HIL technology.

These necessities have an important impact onto the required models for development and test of modern engine control systems. The paper gives an overview about the well know MVEM approach and leads over to a more sophisticated in-cylinder model. Special emphasis is placed on the identical basic equations, e.g. accumulators and valves, in both approaches. The modular setup of the model enables easy exchange of different subsystems. This allows fast implementation and test of new modeling approaches like different heat release functions or wall heat flux models. Three different heat release functions are discussed. During closed loop operation of in-cylinder model and engine control system particular demands with regards to I/O connection have to be fulfilled. Solutions like continuous injection measurement and local oversampling are presented.

Comparison between simulation results and in-cylinder pressure measurement curves show good correlations. But especially during low load engine operation points the lack of an ignition delay model is obvious. This will be regarded in future versions.

The biggest challenge in applying these advanced models in HIL test systems is the automatic model calibration. On the one hand a recursive parameterization process is necessary for in-cylinder models as discussed in [19]. On the other hand the scheduled time for model calibration in today's ECU test system projects is limited. Therefore, a fast parameterization technique is mandatory to achieve good closed loop behaviour in a reasonable project time.

From the authors point of view in-cylinder models will replace the MVEM for HIL testing in the future. Additional sensor information like in-cylinder pressure has to be provided for ECU test systems to satisfy state-of-the-art engine control units. Moreover new actuators (e.g. variable valve train, multiple injection pulses, variable turbine geometry, etc.) increase the number of physical degrees of freedom in combustion engines. Physical based models promise the ability to simulate a reasonable system behavior without the precondition of numerous test bench measurements.

REFERENCES

1. Sommer, A.; Stiegler, L.: „Potential des variablen Ventiltriebs in Pkw-Dieselmotoren“. automotion 01/2006 Page 1, IAV Berlin 2006
2. Jeschke, J.: Konzeption und Erprobung eines zylinderdruckbasierten Motormanagements für PKW-Dieselmotoren: Dissertation. Fakultät für Maschinenbau, Otto-von-Guericke-Universität Magdeburg, Magdeburg 2002
3. Larik, J.: Zylinderdruckbasierte Auflade- und Abgasrückführregelung für PKW-Dieselmotoren: Dissertation. Fakultät für Maschinenbau, Otto-von-Guericke-Universität Magdeburg, Magdeburg 2005
4. Schuette, H.; Ploeger M.: “Hardware-in-the-Loop Testing of Engine Control Units - A Technical Survey”, SAE-Paper 2007-01-0500, 2007
5. Woschni, G.; Fieger, J.: Experimentelle Bestimmung der örtlich gemittelten Wärmeübergangskoeffizienten im Ottomotor. *MTZ* 42, 6 1981, S. 229-234
6. Vibe, I.: Brennverlauf und Kreisprozeß von Verbrennungsmotoren. Verlag Technik, Berlin, 1970
7. Woschni, G.; Anisits, F.: Eine Methode zur Vorausberechnung der Änderung des Brennverlaufes mittelschnellaufender Dieselmotoren bei geänderten Betriebsbedingungen. *MTZ* 34, 4 1973, S. 106-115
8. Friederich, I.; Pucher, H.; Offer, T.: Automatic Model Calibration for Engine –Process Simulation with Heat-Release Prediction. SAE-Paper 2006-01-0655, 2006
9. Philipp, O.; Thalhauser, J.: Ein Dieselmodell mit Abgasturboaufladung, AGR und Zylinderdruckberechnung für HiL und SiL. 5. Symposium: Steuerungssysteme für den Antriebsstrang von Kraftfahrzeugen, Berlin 9.-10. Juni , 2005
10. Chmela, F.; Orthaber, G.: Rate of Heat Release Prediction for Direct Injection Diesel Engines Based on Purely Mixing Controlled Combustion. SAE-Paper 1999-01-0186, 1999
11. Magnussen, B. F.; Hjertager, B. H.: On mathematical modeling of turbulent combustion with special emphasis on soot formation and combustion, 16th Symp. (Int.)on Combust. 1976; 719-729.
12. Lakshinarayanan, P. R.; Aghav, Y. V.; Dani, A. D.; Meta P.S.: Accurate prediction of heat release in a modern direct injection diesel engine. Proceedings of the Institution of Mechanical Engineers / Part D, Journal of automobile engineering, Vol. 216, No. 8, August 2002 S. 663-675
13. Constien, M.: Bestimmung von Einspritz- -und Brennverlauf eines direkteinspritzenden Dieselmotors: Dissertation. Fakultät für Maschinenwesen, TU München, 1991
14. Wolfer, H. H.: Der Zündverzug im Dieselmotor. VDI Forschungsheft 392, 1938
15. Barba C.: Erarbeitung von Verbrennungskennwerten aus Indizierdaten zur verbesserten Prognose und rechnerischen Simulation des Verbrennungsablaufes bei Pkw-DE-Dieselmotoren mit Common-Rail-Einspritzung: Dissertation. Technische Hochschule Zürich, Zürich 2001.
16. Torkzadeh, D.: Echtzeitsimulation der Verbrennung und modellbasierte Reglersynthese am Commom-Rail-Dieselmotor: Dissertation. Fakultät für Elektrotechnik und Informationstechnik, Universität Fridericiana zu Karlsruhe, 2003,
17. Hendricks, E.; Chevalier, A.; Jensen, M.; Spencer, S.; Trumpy, D.; Asik, J.: Modelling of the intake manifold filling dynamics. SAE-Paper 960037, 1996
18. Merker, G. et al.: Verbrennungsmotoren: Simulation der Verbrennung und Schadstoffbildung. Teubner, Wiesbaden: 2. Auflage, 2004
19. Friederich, I.; Pucher, H.; Offer, T.: Automatic Model Calibration for Engine – Process Simulation with Heat-Release Prediction. SAE-Paper 2006-01-0655, 2006
20. Pirker, G.; Chmela, F.; Wimmer, A.: ROHR Simulation for DI Diesel Engines Based on Sequential Combustion Mechanisms. SAE-Paper 2006-01-0654, 2006
21. Beaumont, A.: Hardware in the Loop (HiL) for Engine Control Strategy Development. 3rd biennial dSPACE USA User Conference, Plymouth, MI, 2004
22. Hendricks E.: Mean value modelling of large turbocharged two-stroke diesel engine. SAE Technical Paper 890564, 1989
23. Hendricks, E.; Sorenson, S.C.: Mean Value Modelling of Spark Ignition Engines. SAE Technical Paper No. 90-06-16, 1990.
24. Moskwa, J.J., Hedrick, J.K., Automotive Engine Modeling for Real Time Control Application. Proceedings of the 1987 American Control Conference, WA10-11:00, pp. 341-346, Minneapolis, MN, June 1987.
25. Moskwa, J.J.; Hedrick, J.K.: Modeling and Validation of Automotive Engines for Control Algorithm Development. Transactions of ASME J. of Dynamic Systems, Measurement and Control, Vol. 114, pp. 228-285, June 1992.
26. Hülser, H.; Unger, E.; Neunteufl, K.; Breitegger, B.: Eine zylinderdruckbasierte Motorregelung für niedrigste Emissionen beim Dieselmotor. 5th Symposium control systems for powertrains in vehicles, Berlin, 2005
27. Witthaut, M.: Kurbelwellensynchrones, echtzeitfähiges Modell eines Verbrennungsmotors für Hardware-in-the-Loop Anwendungen: Diplomarbeit, Universität Paderborn, 2005
28. dSPACE GmbH: ASM Diesel Engine Reference, Model Description Version 1.0. Paderborn, 2005
29. dSPACE GmbH: DS 2211 RTI Reference Release 5.0. Paderborn, 2005
30. dSPACE GmbH: DS 2211 HIL I/O Board Features Release 5.0. Paderborn, 2005
31. Heywood, J.: Internal Combustion Engine Fundamentals. McGraw-Hill Book Company, Singapore, 1988

32. Chmela, F.; Orthaber, G.; Schuster, W.: Vorausberechnung des Brennverlaufs von Dieselmotoren mit direkter Einspritzung auf der Basis des Einspritzverlaufs. MTZ 59, 7/8, 1998. S. 484-491
33. Offer, T.: Numerische Lösungskonzepte für die Motorprozeß-Simulation: Dissertation. Fachbereich 11 – Maschinenbau und Produktionstechnik, TU Berlin, 1999
34. Peters, N.: Technische Verbrennung. Vorlesungsskript des Instituts für Technische Mechanik, RWTH-Aachen, 2005
35. Pischinger, R.; Klell, M.; Sams, T.: Thermodynamik der Verbrennungskraftmaschine: Der Fahrzeugantrieb. Springer, Wien; New York, 2. überarbeitete Auflage, 2002
36. Pischinger, R. et al.; List, H. und Pischinger, A. (Hg.): Thermodynamik der Verbrennungskraftmaschine. Neue Folge Band 5 der Reihe Die Verbrennungskraftmaschine, Springer, Wien; New York, 1989
37. ASM - Automotive Simulation Models: Product Information see on http://www.dspace.de/
38. enDyna: Product Information see on: http://www.tesis.de
39. Enginuity: Product Information see on: http://www.simuquest.com
40. Artemis: Information see on http://www.ricardo.com

CONTACT

Dipl.-Ing. Tino Schulze
dSPACE GmbH, Paderborn, Germany
e-mail: tschulze@dspace.de

Dipl.-Ing. Markus Wiedemeier
dSPACE GmbH, Paderborn, Germany
e-mail: mwiedemeier@dspace.de

Dr. Herbert Schuette
dSPACE GmbH, Paderborn, Germany
e-mail: hschuette@dspace.de

Web: http://www.dspace.com

DEFINITIONS, ACRONYMS, ABBREVIATIONS

MVEM: Mean value engine model

ECU: Engine control unit

EGR Exhaust gas recirculation

ROHR: Rate of heat Release

CFD: Computational Fluid Dynamics

VTG Variable Turbine Geometry

VVT Variable Valve Timing

DEFINITIONS

λ	Lambda value
η	Efficiency
η_{λ}	Efficiency function depending on lambda value
η_{Inj}	Efficiency function depending on injection angle
φ	Crank angle
Ψ	Flow function
κ	Isentropic coefficient
ξ	Mass fraction
Π	Pressure ratio
ρ	Gas density
σ_{Fuel}	Fuel surface tension
ω	Engine speed
μ	Discharge coefficient
v	Specific volume
A	Cross section
c_v	Specific heat capacity at constant volume
c_p	Specific heat capacity at constant pressure
c_{Diss}	Diffusion constant
c_{Mod}	Modell constant
c_{Rate}	Mixing rate
c_{Turb}	Conversion constant for turbulent kinetic energy
C	Vibe constant (C = 6.908)
$Ctrl$	Control signal
d	Diameter
E	Energy
E_A	Activation energy
h	Specific enthalpy
H	Enthalpy
i	Factor for a four stroke (i = 0.5) or two stroke (i = 1) engine
J	Inertia Turbocharger
k_R	Reaction rate
l_{Valve}	Valve lift
L_{St}	Stoechiometric constant
m	Mass
n	Shaft speed
n_{Tr}	Number of injected fuel droplets
p	Pressure
P	Cylinder power
q	Specific heat
$q_{Inj,Cyl}$	Injected fuel volume per cylinder

Q	Heat
Q_{LHV}	Lower heating value
Re	Reynolds number
R	Specific gas constant
t	time
T	Temperature
Trq	Torque
u	Specific internal energy
U	Internal energy
V	Volume
We	Weber number
W	Work

SUBSCRIPTS

Acc	Accumulator
Burned	Burned
CD	Combustion duration
Comp	Compressor
Crank	Crankshaft
CS	Combustion start
Cycl	Engine cycle
Cyl	Cylinder
Diff	Diffusion
Diss	Dissipation
Eng	Engine
evap	evapurated
Fuel	Fuel
i	Index of gas components (fuel, air, exhaust)
ID	Ignition delay
Ideal	Nominal value without efficency factor influences
In	Input value
Inj	Injection
InMan	Intake manifold
InValve	Inlet valve
is	isentropic
Kin	kinetic
Mean	Mean value
MeanInd	Mean indicated
Mod	Mdoulated
N	Injector nozzle
Out	Output value
Red	Reduced values
s	Sauter
TC	Turbocharger
Turb	Turbine
vol	volumetric